

See discussions, stats, and author profiles for this publication at: <https://www.researchgate.net/publication/257950653>

A permendur–piezoelectric multiferroic composite for low–noise ultrasensitive magnetic field sensors

Article in *Applied Physics Letters* · April 2012

DOI: 10.1063/1.4705305

CITATIONS

38

READS

306

5 authors, including:



Vladimir Petrov

Novgorod State University

160 PUBLICATIONS 4,152 CITATIONS

SEE PROFILE



Gopalan Srinivasan

Oakland University

446 PUBLICATIONS 14,488 CITATIONS

SEE PROFILE

Some of the authors of this publication are also working on these related projects:



magnetolectric and magnetodielectric structures [View project](#)



core shell process for ferroelectric applications [View project](#)

A permendur-piezoelectric multiferroic composite for low-noise ultrasensitive magnetic field sensors

G. Sreenivasulu, U. Laletin, V. M. Petrov, V. V. Petrov, and G. Srinivasan

Citation: *Appl. Phys. Lett.* **100**, 173506 (2012); doi: 10.1063/1.4705305

View online: <http://dx.doi.org/10.1063/1.4705305>

View Table of Contents: <http://apl.aip.org/resource/1/APPLAB/v100/i17>

Published by the [American Institute of Physics](#).

Related Articles

Variation and sign change of magnetostrictive strain as a function of Ni concentration in Ni-substituted ZnFe₂O₄ sintered nanoparticles

J. Appl. Phys. **111**, 073903 (2012)

Electronic origin of the negligible magnetostriction of an electric steel Fe_{1-x}Si_x alloy: A density-functional study

J. Appl. Phys. **111**, 063911 (2012)

Modeling plastic deformation effect on magnetization in ferromagnetic materials

J. Appl. Phys. **111**, 063909 (2012)

Magnetic and calorimetric studies of magnetocaloric effect in La_{0.7-x}Pr_xCa_{0.3}MnO₃

J. Appl. Phys. **111**, 07D726 (2012)

Converse magnetoelectric effect dependence with CoFeB composition in ferromagnetic/piezoelectric composites

J. Appl. Phys. **111**, 07C725 (2012)

Additional information on *Appl. Phys. Lett.*

Journal Homepage: <http://apl.aip.org/>

Journal Information: http://apl.aip.org/about/about_the_journal

Top downloads: http://apl.aip.org/features/most_downloaded

Information for Authors: <http://apl.aip.org/authors>

ADVERTISEMENT

<p>INSTRUMENTS FOR ADVANCED SCIENCE</p> 	<p>Gas Analysis</p> <p>dynamic measurement of reaction gas streams catalysis and thermal analysis molecular beam studies dissolved species probes fermentation, environmental and ecological studies</p>	<p>Surface Science</p> <p>UHV TPD SIMS end point detection in ion beam etch elemental imaging - surface mapping</p>	<p>Plasma Diagnostics</p> <p>plasma source characterisation etch and deposition process reaction kinetic studies analysis of neutral and radical species</p>	<p>Vacuum Analysis</p> <p>partial pressure measurement and control of process gases reactive sputter process control vacuum diagnostics vacuum coating process monitoring</p>
	<p>contact Hiden Analytical for further details: info@hiden.co.uk www.HidenAnalytical.com</p> <p>CLICK TO VIEW OUR PRODUCT CATALOGUE</p>			

A permendur-piezoelectric multiferroic composite for low-noise ultrasensitive magnetic field sensors

G. Sreenivasulu,¹ U. Laletin,^{1,2} V. M. Petrov,^{1,3} V. V. Petrov,⁴ and G. Srinivasan^{1,a)}

¹Physics Department, Oakland University, Rochester, Michigan 48309, USA

²Institute of Technical Acoustics, National Academy of Sciences of Belarus, 13 Ludnikov Ave., Vitebsk 210023, Belarus

³Institute of Electronic and Information Systems, Novgorod State University, Veliky Novgorod 173003, Russia

⁴Ferrite Domen Company, St. Petersburg 196084, Russia

(Received 17 October 2011; accepted 6 April 2012; published online 23 April 2012)

Low-frequency and resonance magnetolectric (ME) effects have been studied for a trilayer of permendur (alloy of Fe-Co-V) and lead zirconate titanate (PZT). The high permeability and high magnetostriction for permendur, key ingredients for magnetic field confinement, and ME response result in ME voltage coefficient of 23 V/cm Oe at low-frequency and 250 V/cm Oe at electromechanical resonance (EMR) for a sample with PZT fibers and inter-digital-electrodes. Theoretical ME coefficients are in agreement with the data. Measured magnetic noise floor of 25 pT/ $\sqrt{\text{Hz}}$ at 1 Hz and 100 fT/ $\sqrt{\text{Hz}}$ at EMR are comparable to best values reported for Metglas-PZT fiber sensors. © 2012 American Institute of Physics. [<http://dx.doi.org/10.1063/1.4705305>]

A multiferroic is a material that exhibits two or more of primary ferroic properties (ferromagnetism, ferroelectricity, and ferroelasticity).^{1,2} A composite made of ferromagnetic and ferroelectric phases allows for coupling between the electric and magnetic order parameters and, thereby represents an engineered multiferroic.^{3–5} The magnetolectric (ME) coupling in the composite is mediated by mechanical forces. Systems studied so far include ferrites, manganites, or transition metals/alloys for the ferromagnetic phase and barium titanate, polyvinylidene fluoride (PVDF), lead zirconate titanate (PZT), lead magnesium niobate-lead titanate (PMN-PT), or lead zinc niobate-lead titanate (PZN-PT) for the ferroelectric phase.^{1–8} There are recent reports on similar ME composites in which the ferroelectric phase is replaced by a piezoelectric, such as AlN and langatate.^{9,10} The strain-mediated ME coupling is quite strong at room temperature in such composites and has enormous potential for novel functional devices.^{9–19}

This report is on an ultrasensitive multiferroic magnetic sensor with PZT and permendur, an alloy of Fe-Co-V with high effective relative permeability μ_r and high magnetostriction. Data on the observation of pico-tesla sensitivity at low-frequency and femto-tesla sensitivity under resonance conditions are reported in the polarization response of the composite to an applied ac magnetic field. There have been considerable activities in recent years on such ME magnetic sensors that are shown to be passive, operate at room temperature, and can be miniaturized to form an array, and have performance and/or cost advantages over traditional magnetic sensing devices, including superconducting quantum interference device (SQUID), fluxgate, Hall effect, giant magnetoresistance, and magnetic tunnel junctions.^{9–16} The highest sensitivity and lowest noise for ME sensors are reported for composites with Metglas, a ferromagnetic amorphous alloy with high μ_r (required for field confinement) and high piezomagnetic coefficient.^{15–18} Metglas, in general, are available in the form of $\sim 25 \mu\text{m}$ thick ribbons made by rapid

quenching.²⁰ Ribbons of higher thickness, however, are not available due to partial crystallization during synthesis and resulting degradation of magnetic parameters. It is, therefore, necessary to bond several layers of Metglas in an ME sensor to increase the effective thickness of the ferromagnetic layer in order to enhance the sensitivity.^{15,16} Non-magnetic epoxy layers of thickness 2–10 μm used for such bonding are a potential source of demagnetizing fields and noise.

Here, we report on low-frequency and resonance ME coupling and magnetic noise measurements in trilayers of permendur (P), an alloy with 49% Fe, 49% Co, and 2% V, and PZT. The high $\mu_r \sim 2300$ and high magnetostriction λ and piezomagnetic coefficient $q = d\lambda/dH$, for P (Refs. 3 and 21) give rise to a low-frequency magnetolectric voltage coefficient (MEVC) of 1.5 V/cm Oe for P-PZT-P. A fifteen-fold increase in MEVC is measured when the PZT laminate is replaced by PZT fibers with inter-digital-electrodes (IDEs). Enhancement in the MEVC to 250 V/cm Oe is measured when the frequency of ac magnetic field is tuned to longitudinal acoustic modes for the sample. The magnetic floor noise range from 25 pT/ $\sqrt{\text{Hz}}$ at 1 Hz to 100 fT/ $\sqrt{\text{Hz}}$ at resonance. Details of these measurements and comparison with theoretical estimates are provided here.

Permendur (obtained from the Institute of Technical Acoustics, Vitebsk, Belarus) plates of dimensions 8 cm \times 1 cm \times 0.015 cm were used in the study. The permeability and magnetostriction are important parameters for magneto-mechanical coupling in the ferromagnetic phase in the composite and were measured for P. The real part of the relative permeability μ_r' was measured (with an impedance meter and an Agilent Materials Analyzer) over 10 Hz–10 MHz on a toroid of P and the results are shown in Fig. 1. A decrease in μ_r' from 2300 at 10 Hz to 8 at 10 MHz is seen in Fig. 1 and is an order of magnitude smaller than for as-cast Metglas.²⁰ The magnetostriction λ for P was measured with a strain gage. Figure 1 shows data on static field H -dependence of the in-plane λ measured parallel to the field direction. With increasing H , one observes a rapid rise in λ and it saturates at 70 ppm for $H > 200$ Oe. The in-plane λ

^{a)}Email: srinivas@oakland.edu.

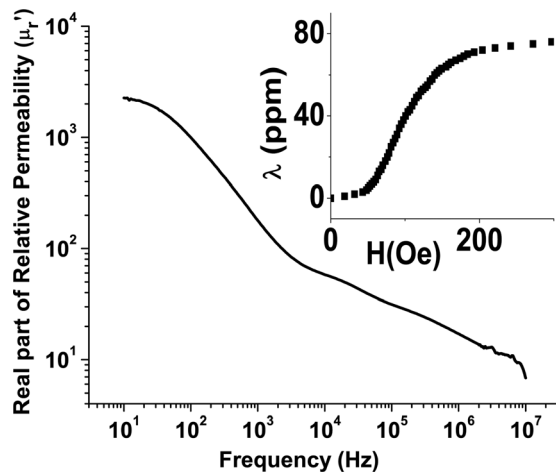


FIG. 1. Real part of the relative permeability μ_r' as a function of frequency for permendur (P). The inset shows the bias field H dependence of the magnetostriction λ measured parallel to the in-plane field for a permendur strip.

perpendicular to H (not shown here) was very small. The piezomagnetic coupling $q = d\lambda/dH$ estimated from the data in Fig. 1 is found to have a maximum value of $1 \times 10^{-6}/\text{Oe}$ for $H = 100$ Oe. It is thus clear from the data in Fig. 1 that permendur is an appropriate choice for use as ferromagnetic phase in ME magnetic sensors. The most important parameter for the ferromagnetic phase is the magneto-mechanical coupling k_m given by $k_m = (4\pi\lambda'\mu_r'/E)^{1/2}$ where λ' is the ac magnetostriction (proportional to q) and E is the Young's modulus.²² For permendur $q\mu_r' \sim 2.3 \times 10^{-3}/\text{Oe}$. For comparison, for Ni with $\mu_r' = 100$ and $q = 0.4 \times 10^{-6}/\text{Oe}$, we obtain $q\mu_r' \sim 0.04 \times 10^{-3}/\text{Oe}$, (Refs. 23 and 24), and for as-cast Metglas ($\mu_r' = 45 \times 10^3$, $q = 1.5 \times 10^{-6}/\text{Oe}$) $q\mu_r' \sim 68 \times 10^{-3}/\text{Oe}$ (Refs. 20 and 24). Thus, $k_m \sim (q\mu_r')^{1/2}$ for P is a factor of 8 higher than for Ni, but is a factor of 5 smaller than for Metglas.

Trilayers of P-PZT-P were made with PZT platelets (American Piezo Ceramics-850)²⁵ or PZT microfiber composites (MFC) encapsulated between layers of IDE and polyamide films (Smart Material Corp.).²⁶ The piezoelectric laminate or MFC was poled in an electric field of 50 kV/cm. Permendur was polished down to 0.15 mm in thickness and was bonded with 2 μm thick epoxy to PZT or MFC. Three types of samples of P-PZT-P were studied: (1) PZT with silver electrodes; (2) PZT with IDE, and (3) MFC with IDE. The overall sample dimensions were $40 \times 10 \times 0.6 \text{ mm}^3$ (PZT plate or MFC of thickness 0.3 mm and P of thickness 0.15 mm each). For ME measurements, the samples were subjected to bias field H and ac field $dH = 1$ Oe, both in-plane and parallel to the length of the sample, and the voltage dV across PZT (or IDE for MFC) was measured with a lock-in-amplifier. The MEVC, $\alpha_E = dV/(t dH)$, where t is the PZT thickness or electrode distance in IDE, was measured as a function of H and frequency f of the ac field. For noise measurements, the sample was placed in a 3-layer mu-metal shielded chamber and subjected to a bias field produced by a pair of barium ferrite permanent magnets and an ac field produced by Helmholtz coils. The sensor output was fed to a low-noise high impedance amplifier (Stanford Research Systems, Model SR560) and then to a spectrum analyzer (Stanford research System, Model SR780).

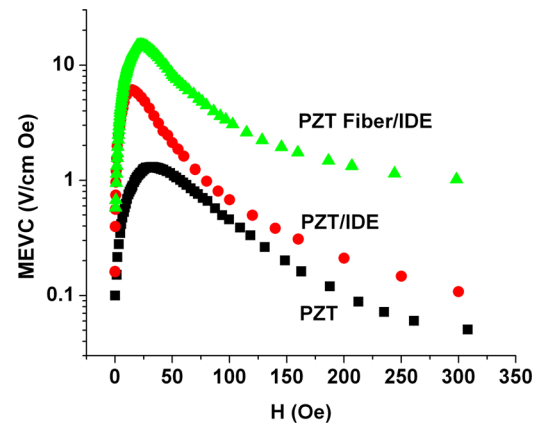


FIG. 2. MEVC vs bias field H measured at 20 Hz for trilayers of permendur and PZT laminate, PZT with IDE, and PZT fibers with IDE.

Figure 2 shows data on MEVC vs H for the trilayers measured for $f = 20$ Hz. A rapid increase in MEVC with H to a maximum is observed for all 3 samples and is followed by a gradual decrease to a minimum for $H > 300$ Oe. The H -variation in MEVC in Fig. 2 essentially tracks the change in q ($= d\lambda/dH$) with the bias magnetic field. The observation of importance is the maximum MEVC of 1.5, 6, and 23 V/cm Oe, respectively, for samples with PZT platelet, PZT with IDE, and PZT fibers with IDE. Thus, a factor of 15 increase in ME sensitivity is achieved when PZT with silver electrodes is replaced by MFC with PZT fibers and IDE. The low-frequency MEVC values in Fig. 2 are orders of magnitude higher than reported values for bulk ferrite-piezoelectric composites, for bilayers and trilayers of ferrite-PZT and lanthanum manganite-PZT (Refs. 3 and 4). The maximum MEVC in Fig. 2 compares favorably with MEVC of 3–52 V/cm Oe at 1 kHz for Metglas composites with PZT fibers and single crystal PMN-PT or PZN-PT. (Refs. 15 and 16).

The frequency dependence of the MEVC was measured for the samples and the results for the sample with MFC are shown in Fig. 3. The bias field was set to the values corresponding to maximum MEVC in Fig. 2. The profile in Fig. 3 shows a resonance in MEVC vs f with a peak MEVC ≈ 250 V/cm Oe at 47 kHz, which is a factor of 10 higher than the maximum MEVC in Fig. 2 for low

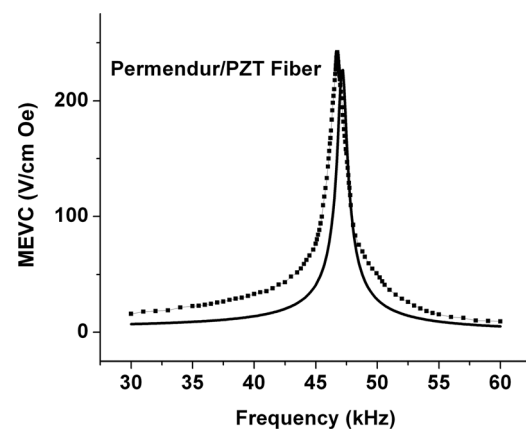


FIG. 3. Frequency dependence of MEVC showing enhancement at EMR for P-PZT fiber-P. The bias field H was set to 25 Oe for maximum in ME response. The peak in MEVC at 47 kHz corresponds to longitudinal acoustic mode in the composite. The solid line represents theoretical estimates.

frequencies. The resonance ME effect is similar in nature to the standard effect, i.e., an induced polarization under the action of an ac magnetic field. But the ac field here is tuned to the longitudinal acoustic frequency. As the ac magnetostriction is responsible for the ME coupling, electromechanical resonance (EMR) at 47 kHz leads to significant increase in the MEVC. The resonance in Fig. 3 has a quality factor $Q=47$. The peak MEVC in Fig. 3 is higher than reported values for trilayers of P with PMN-PT or langatate.¹⁰ Metglas-PMN-PT composites, however, are reported to show a much higher MEVC of ~ 1100 V/cm Oe for EMR at 37.8 kHz. (Ref. 27). A similar resonance corresponding to bending modes occurs in bilayers. Highest MEVC values reported for bending modes are 737 V/cm Oe at 753 Hz for AlN/Fe-Co-Si-B and 720 V/cm Oe at 460 Hz for P-langatate.^{9,10}

Next, we estimate the low-frequency and resonance MEVC for the sample with PZT fibers for comparison with data. Assuming the trilayer in the $(I, 2)$ plane and for the bias and ac magnetic fields and poling field along the length (direction I), the following expression was obtained for the ME voltage coefficient in the low-frequency region:³

$$\alpha_{E,11} = \frac{(q_{11}\nu + q_{12})d_{12} + (q_{12}\nu + q_{11})d_{11}}{d_{11}^2 + d_{12}^2 + 2d_{11}d_{12}\nu - \varepsilon_{11}(1 - \nu^2)(p_{s11} + r^m s_{11})}, \quad (1)$$

$$\bar{\mu} = \frac{m_{s11}\mu_{11}(p_{s11} + r^m s_{11})kL}{\{[r^m s_{11}^2 + (rh_{11}^2\mu_{11} + p_{s11})^m s_{11} + h_{11}^2\mu_{11}p_{s11}]kL - 2h_{11}^2\mu_{11}p_{s11}\tan(\frac{kL}{2})\}},$$

$k = \omega \left[\frac{m_{s11}p_{s11}(r^p\rho + m\rho)}{p_{s11} + r^m s_{11}} \right]^{1/2}$, $h_{11} = q_{11}/\mu_{11}$ with μ_{11} denoting the permeability of the magnetic layer and $m\rho$, and $p\rho$ denoting the density of the magnetic layer and piezoelectric layer, respectively. The above equation was modified for in-plane magnetic fields and poling field.³ Using the values $m\rho = 8.1$ g/cc and $p\rho = 7.7$ g/cc and other parameters given

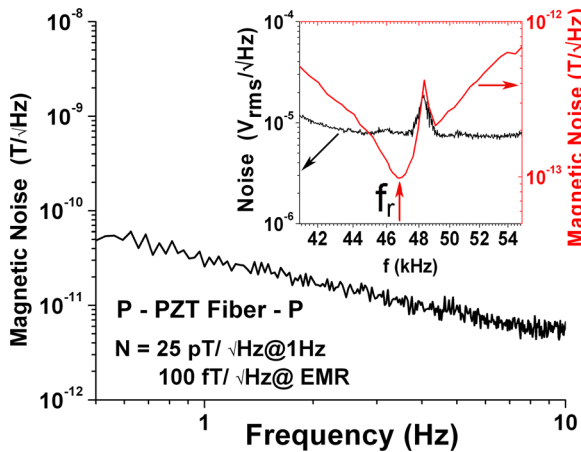


FIG. 4. Magnetic noise at low frequencies for a magnetic sensor of P-PZT fiber-P. The inset shows the voltage noise and magnetic noise as a function of frequency over 41–55 kHz. The sensor output was amplified by a factor of 1000 for these measurements. The lowest noise is measured at EMR and the peak in the data just above EMR is due to environmental noise.

where q_{12} and q_{11} are piezomagnetic coupling coefficients for permendur, d_{12} and d_{11} are piezoelectric coupling coefficients for PZT, ε_{11} is permittivity of PZT, p_{s11} and m_{s11} are compliance coefficient for piezoelectric and magnetostrictive components, ν is Poisson's ratio that is assumed to be equal for all layers for simplicity, and r is the piezoelectric to piezomagnetic layer thickness ratio. The material parameters for PZT fibers are listed below (we used p_{s11} and $\varepsilon_{11}/\varepsilon_0$ for PZT laminates, since the values are not known for the fibers):^{25,26} $d_{11} = 400 \times 10^{-12}$ m/V, $d_{12} = -200 \times 10^{-12}$ m/V, $p_{s11} = 18.5 \times 10^{-12}$ m²/N, $\varepsilon_{33}/\varepsilon_0 = 1850$, $\nu = 0.31$, $q_{11} = 12.4 \times 10^{-9}$ m/A, $q_{12} = -1 \times 10^{-9}$ m/A, $m_{s11} = 7.8 \times 10^{-12}$ m²/N, and $r = 1.0$. Using the above parameters in Eq. (1), one estimates maximum MEVC = 14.4 V/cm Oe, which is 63% of the measured value of 23 V/cm Oe in Fig. 2. Possible causes of this discrepancy are discussed later.

Similarly, an expression for ME voltage coefficient in the EMR region was obtained based on equation of medium motion, material and electrostatic/magnetostatic equations, law of elasticity, and open circuit conditions and is given by

$$\alpha_{E,11} = -\frac{2g_{11}h_{11}\bar{\mu}\tan(kL/2)}{kL(p_{s11} + r^m s_{11})}, \quad (2)$$

where $g_{11} = d_{11}/\varepsilon_{11}$,

earlier for PZT and permendur, we obtained $f_r = 47.2$ kHz and peak MEVC = 220 V/cm Oe (vs measured values of 46.6 kHz and 250 V/cm Oe).

Next, we compare theoretical estimates of ME response at EMR and low-frequency with the data in Figs. 2 and 3. There is very good agreement for the ME response at EMR with deviations of 1% and 10%, respectively, between calculated and measured values of f_r and peak-MEVC. But, there is, however, a much higher deviation between the measured and calculated low-frequency MEVC. The discrepancy could be due to several factors, including the assumption that the Poissons ratio for PZT and permendur are the same in deriving Eq. (1) and the possibility of a spread in the value of parameters for MFC that consisted of several long fibers of PZT. The calculated low-frequency MEVC, in particular, is sensitive to $\varepsilon_{11}/\varepsilon_0$ value. It is noteworthy here that MEVC in Eq. (1) is a function of d_{12} where as the ME coupling at longitudinal EMR is independent of d_{12} . Large variations in $\varepsilon_{11}/\varepsilon_0$ and d_{12} for the fibers could give rise to the poor agreement between theory and data at low-frequency in spite of good agreement at EMR.

Finally, we discuss the magnetic noise measurements for the composites. Data on noise floor were obtained over 0.5 Hz–10 Hz and at EMR. A voltage amplifier with a gain $A_v = 1000$ was used to amplify the sensor output and then fed to a spectrum analyzer. The noise N in terms of T/ $\sqrt{\text{Hz}}$

was estimated from the measured voltage noise (in $V/\sqrt{\text{Hz}}$) and the transfer functions S (in V/T) estimated from data in Figs. 2 and 3. Measured N vs f are shown in Fig. 4 for the sample with PZT fibers. At low frequency, N decreases from 25 $\text{pT}/\sqrt{\text{Hz}}$ at 1 Hz to 7 $\text{pT}/\sqrt{\text{Hz}}$ at 10 Hz. The noise vs f in Fig. 4 shows a peak of unknown origin just above EMR. Several such peaks, possibly due to environmental or electronic noise, were observed in our measurements. The estimated magnetic noise N is down to $\sim 100 \text{ fT}/\sqrt{\text{Hz}}$ at EMR. The low-frequency N for P-PZT fiber is a factor of 80 smaller than for P-PZT and a factor of 5 smaller than for P-PZT with IDE.

Now, we compare the N -values for P-PZT fibers with Metglas based composites. The best N values reported to date are for Metglas based sensors. Gao *et al.* in their work on comparison of sensitivity and noise floor for ME sensors reported N ranging from 20 to 150 $\text{pT}/\sqrt{\text{Hz}}$ (at 10 Hz), respectively, for Metglas with PZT fibers and single crystal PMN-PT or PZN-PT fibers.¹⁵ Wang *et al.* reported a further reduction in N to 5 $\text{pT}/\sqrt{\text{Hz}}$ at 1 Hz for Metglas/PMN-PT fiber sensors.¹⁶ This low-noise for Metglas-based sensors, smaller by a factor 5 than for P-PZT fibers, could be attributed to our earlier observation that the magneto-mechanical coupling k_m for Metglas is higher by a factor of 5 due to high μ_r' . Further improvement in the ME sensitivity and reduction in N for permendur based sensors can be accomplished by high temperature annealing under vacuum or hydrogen in order to increase k_m by increasing μ_r' and q . Permendur samples annealed at 843 °C for 4 h under vacuum and fast cooled to room temperature were found to have μ_r' ranging from 23 000 to 34 000 (vs 45 000 for as-cast Metglas).^{20,21}

In conclusion, studies on magnetoelectric effects on composites of permendur and PZT show a factor 15 improvement in ME sensitivity at low frequency when PZT laminate is replaced by PZT fibers with inter-digital-electrodes. The enhancement in ME sensitivity is attributed to in-plane poling and high piezoelectric coefficient for the PZT fibers. The high ME sensitivity is accompanied by a substantial reduction in noise floor for ME magnetic sensors. The measured N of 25 $\text{pT}/\sqrt{\text{Hz}}$ at 1 Hz and 100 $\text{fT}/\sqrt{\text{Hz}}$ at EMR

for P-PZT fibers are of the same order for the best values reported for Metglas based ME sensors.

The research at Oakland University was supported by grants from the Defense Advanced Research Project Agency (DARPA)—HUMS program and the National Science Foundation.

- ¹W. Eerenstein, N. D. Mathur, and J. F. Scott, *Nature* **442**, 759 (2006).
- ²C. W. Nan, M. I. Bichurin, S. X. Dong, D. Viehland, and G. Srinivasan, *J. Appl. Phys.* **103**, 031101 (2008).
- ³G. Srinivasan, *Ann. Rev. Mater. Res.* **40**, 153 (2010).
- ⁴J. Ma, J. Hu, Z. Li, and C. W. Nan, *Adv. Mater.* **23**, 1062–1087 (2011).
- ⁵G. Lawes and G. Srinivasan, *J. Phys. D: Appl. Phys.* **44**, 243001 (2011).
- ⁶K. Mori and M. Wuttig, *Appl. Phys. Lett.* **81**, 100 (2002).
- ⁷T. Onuta, Y. Wang, C. J. Long, and I. Takeuchi, *Appl. Phys. Lett.* **99**, 203506 (2011).
- ⁸V. Castel and C. Brosseau, *Appl. Phys. Lett.* **92**, 233110 (2008).
- ⁹H. Greve, E. Woltermann, H. Quenzer, B. Wagner, and E. Quandt, *Appl. Phys. Lett.* **96**, 182501 (2010).
- ¹⁰G. Sreenivasulu, L. Y. Fetisov, Y. K. Fetisov, and G. Srinivasan, *Appl. Phys. Lett.* **100**, 052901 (2012).
- ¹¹Y. Fetisov, A. Bush, K. Kametsev, A. Ostashchenko, and G. Srinivasan, *IEEE Sensors* **6**, 935 (2006).
- ¹²S. Priya, R. Bergs, and R. A. Islam, *J. Appl. Phys.* **101**, 024108 (2007).
- ¹³M. Vopsariou, J. Blackburn, and M. G. Cain, *J. Phys. D: Appl. Phys.* **40**, 5027 (2007).
- ¹⁴J. Lenz and A. S. Edelstein, *IEEE Sensors* **6**, 631 (2006).
- ¹⁵J. Gao, J. Das, Z. Xing, J. Li, and D. Viehland, *J. Appl. Phys.* **108**, 084509 (2010).
- ¹⁶J. Wang, D. Gray, D. Barry, J. Gao, M. Li, J. Li, and D. Viehland, *Adv. Mater.* **23**, 4111 (2011).
- ¹⁷C. Park, D. Avirovik, S. Bressers, and S. Priya, *Appl. Phys. Lett.* **98**, 062904 (2011).
- ¹⁸Y. Chen, S. Gillette, T. Fitchorov *et al.*, *Appl. Phys. Lett.* **99**, 042505 (2011).
- ¹⁹P. Zhao, Z. Zhao, D. Hunter, R. Suchoski, C. Gao, S. Mathews, M. Wuttig, and I. Takeuchi, *Appl. Phys. Lett.* **94**, 243507 (2009).
- ²⁰Tech. Bulletin ref:2605SA106192009 (Metglas Inc., Conway, SC), 2009.
- ²¹R. E. Burket and D. M. Stewart, *J. Appl. Phys.* **33**, 1224 S (1962).
- ²²C. M. Van der Burgt, *Philips Res. Rep.* **8**, 91 (1953).
- ²³D. Jiles, *Introduction to Magnetism and Magnetic Materials* (CRC Taylor & Francis, New York, 1998), p. 97.
- ²⁴G. Sreenivasulu, S. Bandekar, V. M. Petrov, and G. Srinivasan, *Phys. Rev. B* **84**, 144426 (2011).
- ²⁵Sample used: NAVY-II: APC 850, *Physical and Piezoelectric Properties* (APC International, Mackyville, PA), 2009.
- ²⁶Sample used: MFC-P1, *Microfiber Composite Data Sheet* (Smart Material Corp., Sarasota, FL), 2012.
- ²⁷J. Gao, L. Shen *et al.*, *J. Appl. Phys.* **109**, 074507 (2011).